Calculation of stresses and slips in flexible armour layers with layers interaction

Article · January 1995

CITATIONS
36

READS
327

3 authors, including:

Jean-Marc Leroy
IFP Energies nouvelles
21 PUBLICATIONS **224** CITATIONS

SEE PROFILE

1995 OMAE – Volume V, Pipeline Technology
ASME 1995

CALCULATION OF STRESSES AND SLIPS IN FLEXIBLE ARMOUR LAYERS WITH LAYERS INTERACTION.

Jany Féret and Jean-Marc Leroy
Institut Français du Pétrole
Rueil-Malmaison
France

Pascal Estrier
Coflexip
Le Trait
France

ABSTRACT

This paper deals with stress and displacement calculation in dynamically bent unbonded flexible pipes. The presented method is original in that movements and stresses of both armour layers are coupled. Good correlations between strain measurements and the theory have been found, as shown in the paper.

INTRODUCTION

Design life prediction of flexible risers is of outstanding importance to ensure reliability of offshore structures.

In a simplified manner, a flexible riser design is an iterative three-step procedure:

- a first analysis gives the static behaviour of the flexible pipe components under axial tension, internal and external pressure,
- a second analysis determines dynamic tension and curvature variations along the pipe according to environmental conditions (waves, current, vessel motions, ...),
- a third analysis determines stresses and slips in pipe layers due to curvature variations.

This paper deals with the third step, as Coflexip has requested I.F.P. to carry out a study on variations of stresses and slips of flexible pipe components (mainly of tensile armour layers) in dynamic bending to predict fatigue and wear.

Most of existing methods assume the shape of the deformed armours (Féret et al, 1987, Féret et al, 1989) or only consider one armour layer (Sævik, 1992). The method presented in this paper is an improvement in unbonded flexible pipes design as movements and loads in both tensile armour layers are considered.

Coflexip flexible pipes designs are based on a former state of the theory (Estrier, 1992). However, they are carefully correlated with representative fatigue tests and have always been found conservative. This improved theory then allows better understanding of flexible pipes behaviour.

The method is described in two steps. The first is a geometrical analysis of deformed helices on a torus, where basic equations between curvatures and displacements are obtained. In the second step, friction and equilibrium equations are presented. A system of differential equations that links displacements and forces of both armour layers is obtained.

Numerical examples of armours displacements and friction effects are then presented.

The paper ends with a comparison between theoretical results and strain measurements.

NOMEMCLATURE

a	radius of armour layers
C_b, C_n	transverse and normal curvatures of a curve
F_t	tangential force in an armour
$\vec{q}$	friction force (per unit length of a helix) between the substrate and the internal armour layer
$\vec{Q}$	friction force (per unit length of a helix) between the internal and the external helices
R	radius of curvature of the pipe
s	curvilinear abscissa along a helix
$\vec{t}$	unit tangential vector of a curve
$\vec{N}$	unit vector normal to the bent pipe
$\vec{B}$	unit transverse vector of a curve
x_1, x_2, x_3	rectangular coordinates of a point of a torus
α	initial laying angle of a helix
Δ_t, Δ_b	slip of a point of a helix relatively to the torus, respectively in $\vec{t}$ and $\vec{B}$ directions
δ_t^e, δ_b^e	slip of a point of an external helix relatively to the internal helix, respectively in $\vec{t}^{\,e}$ and $\vec{B}^e$ directions

$\varepsilon = \frac{a}{R}$	relative curvature of the pipe
θ, φ	angular coordinates of a point of a torus
$\frac{1}{\tau}$	torsion of a curve
σ	stress
Subscripts:	
t	in tangential direction
b	in transverse direction
Superscript:	
e	relative to the external armour layer

GEOMETRICAL ANALYSIS

A curve on a bent pipe can be defined in Darboux-Ribeaucourt axes $(\vec{t}, \vec{N}, \vec{B})$, where $\vec{t}$ is the unit tangential vector, $\vec{N}$ is the unit internal normal to the bent pipe, $\vec{B} = \vec{t} \Lambda \vec{N}$ is in the transverse direction.
If S is the curvilinear abscissa along the curve, then:

$$\begin{bmatrix} \frac{d\vec{t}}{ds} \\ \frac{d\vec{N}}{ds} \\ \frac{d\vec{B}}{ds} \end{bmatrix} = \begin{bmatrix} 0 & C_n & C_b \\ -C_n & 0 & -\frac{1}{\tau} \\ -C_b & \frac{1}{\tau} & 0 \end{bmatrix} \begin{bmatrix} \vec{t} \\ \vec{N} \\ \vec{B} \end{bmatrix} \quad (1)$$

where C_b, C_n are respectively transverse and normal curvatures and $\frac{1}{\tau}$ is the torsion of the curve.

Assuming that the bent pipe (of radius a) is a torus of constant radius of curvature R (figure 1), a point M on the torus has the following coordinates in $(\vec{i}, \vec{j}, \vec{k})$ axes:

$$\begin{aligned} x_1 &= (R + a.\cos\theta).\cos\varphi \\ x_2 &= (R + a.\cos\theta).\sin\varphi \\ x_3 &= a.\sin\theta \end{aligned} \quad (2)$$

As:

$$(ds)^2 = (dx_1)^2 + (dx_2)^2 + (dx_3)^2 \quad (3)$$

$$\vec{t} = \frac{dx_1}{ds}\vec{i} + \frac{dx_2}{ds}\vec{j} + \frac{dx_3}{ds}\vec{k} \quad (4)$$

$$\vec{N} = -\cos\theta.\cos\varphi.\vec{i} - \cos\theta.\sin\varphi.\vec{j} - \sin\theta.\vec{k} \quad (5)$$

$\frac{ds}{d\theta}, C_b, C_n, \frac{1}{\tau}$ can be deduced from equations (1) to (5):

$$\left(\frac{ds}{d\theta}\right)^2 = a^2 + R^2.v^2.g^2 \quad (6)$$

$$C_b = \left[\sin\theta.\left(2.a^2.g + R^2.v^2.g^3\right) - a.R.v.\frac{dg}{d\theta}\right]\left(\frac{d\theta}{ds}\right)^3 \quad (7)$$

$$C_n = \left[a + R.v.\cos\theta.g^2\right]\left(\frac{d\theta}{ds}\right)^2 \quad (8)$$

$$\frac{1}{\tau} = R.g.\left(\frac{d\theta}{ds}\right)^2 \quad (9)$$

where: $g = \frac{d\varphi}{d\theta}, \varepsilon = \frac{a}{R}, v = 1 + \varepsilon.\cos\theta$

Hence curves on the torus are completely defined if (for example) $g = \frac{d\varphi}{d\theta}$ is given.

It is assumed that the deformed helices can be described by:

$$\frac{d\varphi}{d\theta} = \frac{\varepsilon}{tg\alpha}(1 + z.\varepsilon.\cos\theta) \quad (10)$$

where: ε is supposed to be small,
α: initial laying angle of the helix,
z a constant.

The choice of equation (10), applying in the current length of the pipe, was governed by previous studies of well-known curves on a surface, such as the geodesic or the loxodromic curves.

Introducing equation (10) into equations (6,7,8), the following results are obtained (refer to appendix 1 for mathematical developments):

$$\Delta_b = -a.\cos\alpha.z.\varepsilon.\sin\theta \quad (11)$$

$$\Delta_t = -a.\frac{\cos^2\alpha}{\sin\alpha}.\varepsilon.\sin\theta \quad (12)$$

$$\Delta C_n = \frac{\cos^2\alpha}{a}.\left(\cos 2\alpha - 2z.\sin^2\alpha\right).\varepsilon.\cos\theta \quad (13)$$

$$\Delta C_b = \frac{\cos\alpha}{a}.\left(1 + \sin^2\alpha + z.\sin^2\alpha\right).\varepsilon.\sin\theta$$

$$\text{or } \Delta C_b = \frac{\varepsilon}{a}.\cos\alpha.\left(1 + \sin^2\alpha\right).\sin\theta - \frac{\sin^2\alpha}{a^2}.\Delta_b \quad (14)$$

where:

Δ_t (respectively Δ_b) is the slip of a point of the helix relatively to the torus in the tangential (respectively transverse) direction,

$\Delta C_b, \Delta C_n$ are variations of transverse and normal curvatures with respect to the undeformed straight pipe.

Note that the elastic displacement due to friction was neglected when compared to geometrical displacement to obtain the previous expression of Δ_t.

MECHANICAL ANALYSIS

The studied flexible pipe is made of two armour layers of equal and opposite laying angles ($\pm\alpha$). The internal layer is supported by a substrate that is modeled as a cylinder. We define:
- a : the radius of armour layers, assumed to be the same that the radius of the substrate,
- R : the constant radius of curvature of the bent substrate,
- $\vec{q}$: the friction force (per unit length of a helix) at the interface between the substrate and the internal armour layer,
- $\vec{Q}$: the friction force (per unit length of a helix) at the interface between the two armour layers.

$\vec{q}$ and $\vec{Q}$ are supposed to be constant.

Quantities relative to the external armour layer are noted with a superscript (^{e}). For example, Δ_t^e is the slip of an external helix

(relatively to the substrate) in the direction of $\vec{t}^{\,e}$, tangent vector of the external helix.

Note that the slip of an external helix relatively to an internal helix is defined as $\vec{\delta}^{e}$, with:

$$\begin{aligned}\delta_b^e &= \vec{\delta}^e.\vec{B}^e = \Delta_b^e - \left(\Delta_b.\cos 2\alpha + \Delta_t.\sin 2\alpha\right)\\ \delta_t^e &= \vec{\delta}^e.\vec{t}^{\,e} = \Delta_t^e - \left(-\Delta_b.\sin 2\alpha + \Delta_t.\cos 2\alpha\right)\end{aligned} \tag{15}$$

Equations of friction

When sliding occurs, friction forces are opposed to the sliding velocity. Equations of friction can be written as:

- at a point q of a helix of the external armour layer:

$$\frac{\dfrac{\partial \delta_b^e}{\partial \varepsilon}}{\dfrac{\partial \delta_t^e}{\partial \varepsilon}} = \frac{Q_b^e}{Q_t^e} \tag{16}$$

with:

$$Q_b^e = \vec{Q}.\vec{B}^e, \quad Q_t^e = \vec{Q}.\vec{t}^{\,e}, \quad \left(Q_t^e\right)^2 + \left(Q_b^e\right)^2 = Q^2,$$

$$Q_b^e.\frac{\partial \delta_b^e}{\partial \varepsilon} < 0, \quad Q_t^e.\frac{\partial \delta_t^e}{\partial \varepsilon} < 0$$

- at a point q of a helix of the internal armour layer:

$$\frac{\dfrac{\partial \Delta_b}{\partial \varepsilon}}{\dfrac{\partial \Delta_t}{\partial \varepsilon}} = \frac{q_b}{q_t} \tag{17}$$

with:

$$q_b = \vec{q}.\vec{B}, \quad q_t = \vec{q}.\vec{t}, \quad \left(q_t\right)^2 + \left(q_b\right)^2 = q^2,$$

$$q_b.\frac{\partial \Delta_b}{\partial \varepsilon} < 0, \quad q_t.\frac{\partial \Delta_t}{\partial \varepsilon} < 0$$

Equilibrium equations

Equilibrium of a length ds of a helix of the external armour layer gives, when neglecting shear forces:

$$\left(F_t^e + dF_t^e\right).\left(\vec{t}^{\,e} + d\vec{t}^{\,e}\right) - F_t^e.\vec{t}^{\,e} + \vec{Q}.ds = 0 \tag{18}$$

where F_t^e is the tangential (or axial) force in the armour.

Then:

.in $\vec{t}^{\,e}$ direction: $$\frac{dF_t^e}{ds} + Q_t^e = 0 \tag{19}$$

.in $\vec{B}^e$ direction (as $\frac{d\vec{t}^{\,e}}{ds}.\vec{B}^e = \Delta C_b^e$): $F_t^e.\Delta C_b^e + Q_b^e = 0$ (20)

Equilibrium of a length ds of a helix of the internal armour layer (submitted to both distributed loads $\vec{q}$ and $-\vec{Q}$) gives, when neglecting shear forces:

$$\left(F_t + dF_t\right).\left(\vec{t} + d\vec{t}\right) - F_t.\vec{t} + \vec{q}.ds - \vec{Q}.ds = 0 \tag{21}$$

Then:

.in $\vec{t}$ direction: $$\frac{dF_t}{ds} + q_t - Q_t^e.\cos 2\alpha - Q_b^e.\sin 2\alpha = 0 \tag{22}$$

.in $\vec{B}$ direction (as $\frac{d\vec{t}}{ds}.\vec{B} = \Delta C_b$):

$$F_t.\Delta C_b + q_b + Q_t^e.\sin 2\alpha - Q_b^e.\cos 2\alpha = 0 \tag{23}$$

Note that F_t^e (respectively F_t) is the sum of a force F_P due to pressure in the pipe (F_P can be considered equal in internal and external helices) and a force F_F^e (respectively F_F) due to friction .

Resolution

The problem is solved in two steps:

- in the first step, axial deformation induced by friction is neglected. Then set of equations (11) to (14) is used and:

$$F_t.\Delta C_b \cong F_P.\Delta C_b, \quad F_t^e.\Delta C_b^e \cong F_P.\Delta C_b^e$$

Equations (15), (16), (17), (19), (20), (22) and (23) are reduced to the following system of differential equations:

$$\frac{\dfrac{\partial \Delta_b^e}{\partial \varepsilon} - \left(\dfrac{\partial \Delta_b}{\partial \varepsilon}.\cos 2\alpha + \dfrac{\partial \Delta_t}{\partial \varepsilon}.\sin 2\alpha\right)}{\dfrac{\partial \Delta_t^e}{\partial \varepsilon} - \left(-\dfrac{\partial \Delta_b}{\partial \varepsilon}.\sin 2\alpha + \dfrac{\partial \Delta_t}{\partial \varepsilon}.\cos 2\alpha\right)} = \frac{\varsigma}{\pm\sqrt{Q^2 - \varsigma^2}} \tag{24}$$

$$\frac{\dfrac{\partial \Delta_b}{\partial \varepsilon}}{\dfrac{\partial \Delta_t}{\partial \varepsilon}} = \frac{\gamma}{\pm\sqrt{q^2 - \gamma^2}} \tag{25}$$

with:

$$\varsigma = F_P.\Delta C_b^e$$

$$\gamma = F_P.\Delta C_b + \sqrt{Q^2 - \left[F_P.\Delta C_b^e\right]^2}\,\sin 2\alpha - F_P.\Delta C_b^e\,\cos 2\alpha$$

and:

$$\Delta_t = -a.\frac{\cos^2\alpha}{\sin\alpha}.\varepsilon.\sin\theta = -\Delta_t^e$$

$$\Delta C_b = \frac{\varepsilon}{a}\cos\alpha\left(1 + \sin^2\alpha\right).\sin\theta - \frac{\sin^2\alpha}{a^2}\Delta_b$$

$$\Delta C_b^e = \frac{\varepsilon}{a}\cos\alpha\left(1 + \sin^2\alpha\right).\sin\theta - \frac{\sin^2\alpha}{a^2}\Delta_b^e$$

As $\Delta_t, \Delta_b, \Delta_t^e, \Delta_b^e$ have sinusoïdal shapes, the previous system can be numerically solved only in $\theta = \frac{\pi}{2}$, with a second-order Runge-Kutta method. Equations (24) and (25) show that both armour layers displacements are coupled.

- in the second step, tangential friction forces are deduced from equations (19) and (22), with q_t, q_b, Q_t^e, Q_b^e calculated in first step, and $F_t\left(\theta = \frac{\pi}{2}\right) = 0$, $F_t^e\left(\theta = \frac{\pi}{2}\right) = 0$ by symmetry.

Hence maximal axial stresses at a point θ are:

- in the internal helix:

$$\sigma_t(\theta)=\frac{F_P}{A}+E\frac{e}{2}\Delta C_n(\theta)+E\frac{h}{2}\Delta C_b(\theta)+\frac{q_t a}{A\sin\alpha}\left(\frac{\pi}{2}-\theta\right),$$

with E,A,e,h respectively the Young's modulus, the section, the thickness and the width of the internal helix.

- in the external helix:

$$\sigma_t^e(\theta)=\frac{F_P}{A^e}+E^e\frac{e^e}{2}\Delta C_n^e(\theta)+E^e\frac{h^e}{2}\Delta C_b^e(\theta)+\frac{Q_t^e a}{A^e\sin\alpha}\left(\frac{\pi}{2}-\theta\right)$$

with E^e,A^e,e^e,h^e respectively the Young's modulus, the section, the thickness and the width of the external helix.

THEORETICAL EXAMPLES

In this section, a flexible pipe (a = 0.1 m, α = 35°, $E=E^e=2.10^{11}$ Pa, $A=A^e=25.10^{-6}\,m^2$, $e=e^e=3.10^{-3}$ m, $h=h^e=9.10^{-3}$ m) is subjected to cycles of curvature from $\frac{1}{R}$ = 0 to $\frac{1}{R}=0.3\ m^{-1}$, with $F_P=3600$ N.

In figure 2, movements of internal and external helices ($\theta=\frac{\pi}{2}$) are represented (Δ_b versus Δ_t for the internal helix, δ_b^e versus δ_t^e for the external helix), with $q=2Q=1300$ N/m. Figure 2 shows that a steady cycle of movement is obtained for each helix after only a few cycles of variation of curvature of the pipe. Steady cycles occur around geodesic curves (represented in dotted lines in figure 2) and are centered on half the amplitude of geodesic displacements. In this example, amplitudes of steady displacements are much lower than amplitudes of displacements of geodesic curves.

In figures 3 to 6, the steady cycle is studied when friction forces are varied. At $\theta=\frac{\pi}{2}$, figures 3 and 4 show that variations of transverse curvature of the internal helix are little affected by studied friction forces, when variations of transverse curvature of the external helix greatly depend on friction. Steady cycles are also centered around the geodesic curve as $\Delta C_b=\Delta C_b^e=0$ when $\frac{1}{R}=0.15\ m^{-1}$. Axial stress variations at $\theta=0$ are plotted in figures 5 and 6. Maximum axial stress variations are not obtained with maximum friction forces, especially in the external helix, as the contribution of normal curvature variation can be higher than the contribution of friction. Note that axial stress variations can be lower in the internal helix than in the external helix, depending on studied friction.

THEORY-EXPERIMENTS COMPARISON

A 6" internal diameter Coflexip flexible pipe of 8 m in length was tested on a dynamic bench test. Both end-fittings of the flexible pipe can rotate and one end-fitting can translate. Imposed rotations and translation were chosen to obtain (as far as possible) constant variations of curvature along the pipe. Figure 7 is an example of the flexible pipe movement.

Windows were cut in the external sheath at the pipe center and strain gauges were stuck on the external armour layer, at $\theta=0$ (extrados), $\theta=\frac{\pi}{2}$ (neutral bending axis) and $\theta=\pi$ (intrados). Parallel strain gauges were used to obtain both axial and transverse strain variations.

Six test results (three internal pressure: 50, 100 and 150 bar and two variations of curvature: $\Delta\left(\frac{1}{R}\right)\cong 0.025\ m^{-1}$ and $\Delta\left(\frac{1}{R}\right)\cong 0.07\ m^{-1}$) have been compared with theory.

Theoretical results were obtained as following:

- the force F_P due to pressure and the ratio $\frac{Q}{q}$ were determined with dedicated computer program (Féret et al, 1987),
- experimental data at extrados and intrados, when direction of curvature variation changes, were used to determine the friction force Q,
- measured curvature variations on the bench test were used in theoretical simulations.

Theoretical and experimental variations of axial stress ($\theta=0$ or $\theta=\pi$) and transverse bending stress ($\theta=\frac{\pi}{2}$) were compared. In both cases the relative error is the the range of 10 to 15% and do not exceed 20%.

Figures 8 and 9 are comparison between theoretical and experimental cycles. Shapes of both axial and transverse strain variations are well predicted by theory.

The presented theory is then in good agreement with experimental measurements.

CONCLUSION

A method of dynamic stress and displacement calculation in flexible pipelines has been presented. It is based on geometrical, friction and equilibrium equations in both tensile armour layers. Good correlation has been found with strain measurements. When the flexible pipe is bent with cycles of curvature of constant amplitude, a steady state is obtained around the geodesic curve.

REFERENCES

Estrier, P., 1992, "Updated Method for the Determination of the Service Life of Flexible Risers", Proceedings of the First European Conference Marinflex.

Féret, J., and Bournazel, C., 1987, "Calculation of Stresses and Slip in Structural Layers of Unbonded Flexible Pipes", Journal of Offshore Mechanics and Artic Engineering,, Vol. 109, pp. 263-269.

Féret, J., and Momplot, G., 1989, "Caflex, Computer Program for Capacity Analysis of Flexible pipes", I.F.P. - SINTEF Structural Engineering report, n° STF71 F91019.

Sævik, S., 1992, "On Stresses and Fatigue in Flexible Pipes", Dr. Ing. These, University of Trondheim.

APPENDIX 1

From: $\left(\frac{ds}{d\theta}\right)^2 = a^2 + R^2.v^2.g^2$ and:

$g = \frac{d\varphi}{d\theta} = \frac{\varepsilon}{tg\alpha}(1 + z.\varepsilon.\cos\theta)$, when neglecting terms in $\varepsilon^2, \varepsilon^3, \ldots$: $\frac{ds}{d\theta} = \frac{a}{\sin\alpha}\left[1 + (z+1).\cos^2\alpha.\varepsilon.\cos\theta\right]$.

If a point M is repered with $\theta = \theta_0, s = s_0 = \frac{a\theta_0}{\sin\alpha}$ when $\varepsilon = 0$ (straight pipe) and $\theta = \theta_\varepsilon, s = s_\varepsilon$ when $\varepsilon \neq 0$ (bent pipe), then:

$$s_\varepsilon - s_0 = \int_0^{\theta_\varepsilon} \frac{ds}{d\theta} d\theta - \frac{a\theta_0}{\sin\alpha}$$

$$= \frac{a}{\sin\alpha}\left[\theta_\varepsilon - \theta_0 + (1+z).\cos^2\alpha.\varepsilon.\sin\theta_\varepsilon\right]$$

$$= \frac{\Delta_C}{\sin\alpha} + \frac{a}{\sin\alpha}(1+z).\cos^2\alpha.\varepsilon.\sin\theta_\varepsilon$$

where $\Delta_C = a.(\theta_\varepsilon - \theta_0)$ is the displacement of M (relatively to the torus) along a meridian (φ constant).

Let introduce Δ_p the displacement of M along a parallel (θ constant):

$$\Delta_p = (R + a.\cos\theta)\left[\int_0^{\theta_\varepsilon} \frac{d\varphi}{d\theta} d\theta - \frac{\varepsilon\theta_0}{tg\alpha}\right]$$

As $\frac{d\varphi}{d\theta} = \frac{\varepsilon}{tg\alpha}(1 + z.\varepsilon.\cos\theta)$,:

$$\Delta_p \cong \frac{a}{tg\alpha}(1 + \varepsilon.\cos\theta)\left[\theta_\varepsilon - \theta_0 + z.\varepsilon.\sin\theta_\varepsilon\right]$$

or: $z.\varepsilon.\sin\theta_\varepsilon = \frac{tg\alpha}{a}\Delta_p - \frac{\Delta_C}{a}$.

Then:

$$s_\varepsilon - s_0 \cong \sin\alpha.\Delta_C + \cos\alpha.\Delta_p + \frac{a}{\sin\alpha}.\cos^2\alpha.\varepsilon.\sin\theta_\varepsilon$$

$$\cong \Delta_t + \frac{a}{\sin\alpha}.\cos^2\alpha.\varepsilon.\sin\theta_\varepsilon$$

If axial deformation is neglected, $s_\varepsilon - s_0 = 0$ and:

$$\Delta_t(\theta) = -\frac{a}{\sin\alpha}.\cos^2\alpha.\varepsilon.\sin\theta.$$

Note that:

$$z.\varepsilon.\sin\theta_\varepsilon = \frac{tg\alpha}{a}\Delta_p - \frac{\Delta_C}{a}$$

$$= \frac{1}{a.\cos\alpha}\left(\sin\alpha.\Delta_p - \cos\alpha.\Delta_C\right) = -\frac{\Delta_b}{a.\cos\alpha}$$

or: $\Delta_b(\theta) = -a.\cos\alpha.z.\varepsilon.\sin\theta$

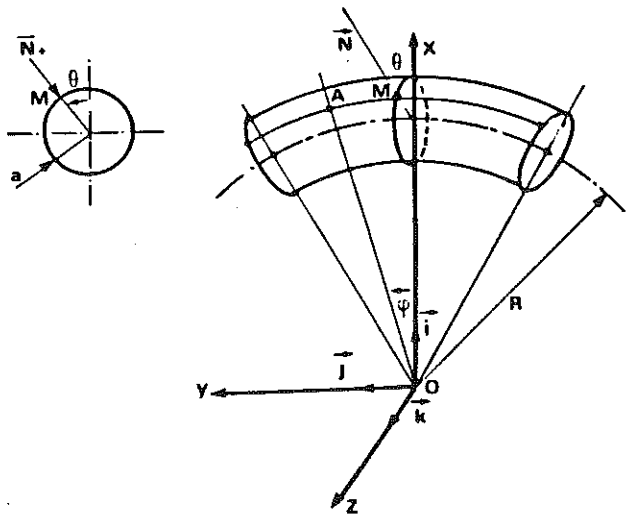

Figure 1 - Mathematical parameters definition

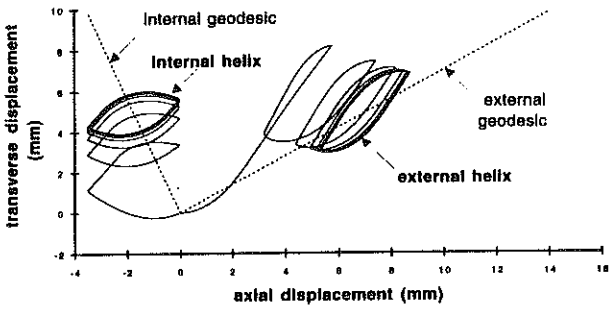

Figure 2 - Trajectories of helices (Δ_b versus Δ_t for the internal helix, δ_b^e versus δ_t^e for the external helix) in cycles of curvature, when $\theta = \frac{\pi}{2}$ and $q = 2Q =$ 1300 N/m. In dotted lines: trajectories of geodesic curves.

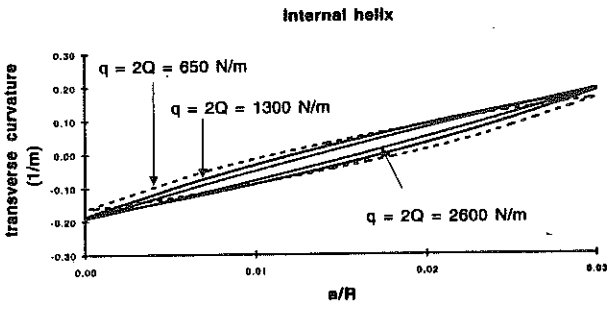

Figure 3 - Transverse curvature of the internal helix versus relative curvature $\frac{a}{R}$, ($\theta = \frac{\pi}{2}$, steady cycle)

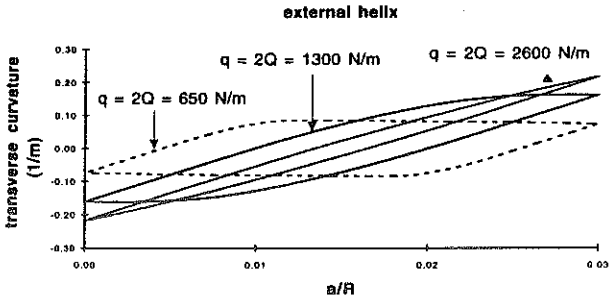

Figure 4 - Transverse curvature of the external helix versus relative curvature $\frac{a}{R}$, ($\theta = \frac{\pi}{2}$, steady cycle)

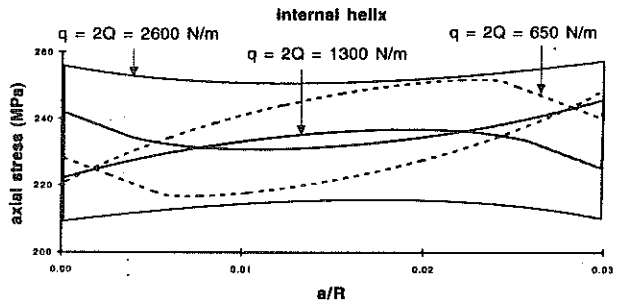

Figure 5 - axial stress of the internal helix versus relative curvature $\frac{a}{R}$, ($\theta = 0$, steady cycle)

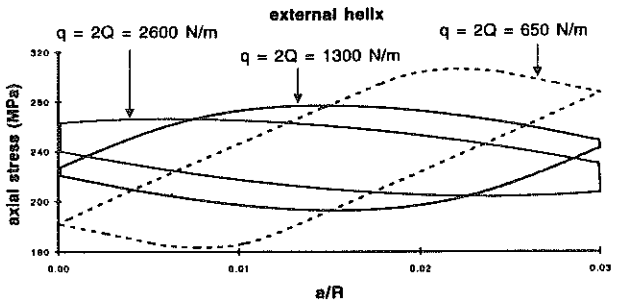

Figure 6 - axial stress of the external helix versus relative curvature $\frac{a}{R}$, ($\theta = 0$, steady cycle)

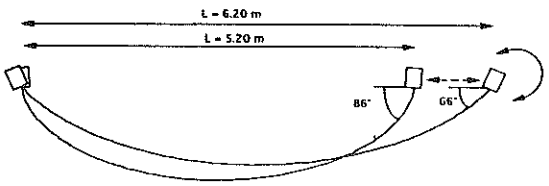

Figure 7 - example of displacements and rotations imposed on the pipe in the bench test.

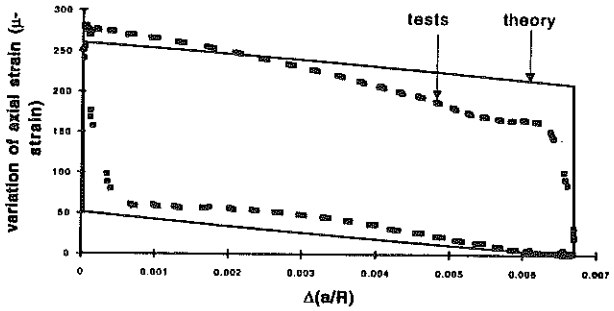

Figure 8 - comparison of measured and theoretical variations of axial strain ($\theta = 0$, steady cycle)

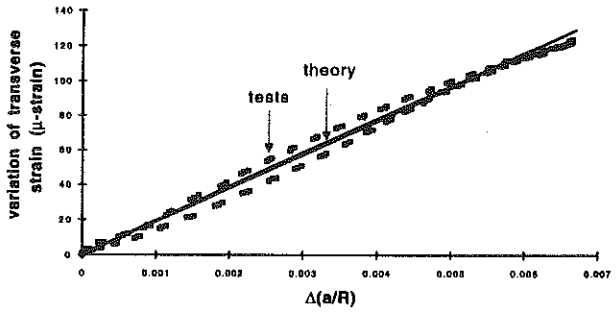

Figure 9 - comparison of measured and theoretical variations of transverse bending strain ($\theta = \frac{\pi}{2}$, steady cycle)